Bergische Universität Wuppertal

Fakultät für Mathematik und Naturwissenschaften

Institute of Mathematical Modelling, Analysis and Computational Mathematics (IMACM)

M. Clemens, F. Kasolis, M.-L. Henkel, B. Kähne, and M. Günther

A Two-Step Darwin Model Time Domain Formulation for Quasistatic Electromagnetic Field Calculations

February 8, 2021

http://www.imacm.uni-wuppertal.de

A Two-Step Darwin Model Time Domain Formulation for Quasistatic Electromagnetic Field Calculations

M. Clemens[1], F. Kasolis[1], M.-L. Henkel[1], B. Kähne[1], and M. Günther[2]

Institute of Mathematical Modelling, Analysis and Computational Mathematics IMACM, University of Wuppertal,

[1] Chair of Electromagnetic Theory, Rainer-Gruenter-Straße 21, 42119 Wuppertal, Germany

[2] Chair of Numerical Analysis and Applied Mathematics, Gaußstraße 20, 42119 Wuppertal, Germany

In the absence of wave propagation, transient electromagnetic fields are governed by a composite scalar/vector potential formulation for the quasistatic Darwin field model. Darwin-type field models are capable of capturing inductive, resistive, and capacitive effects. To avoid possibly non-symmetric and ill-conditioned fully discrete monolithic formulations, here, a Darwin field model is presented which results in a two-step algorithm, where the discrete representations of the electric scalar potential and the magnetic vector potential are computed consecutively. Numerical simulations show the validity of the presented approach.

Index Terms—Computational electromagnetics, electromagnetic fields, numerical simulation, time domain analysis.

I. INTRODUCTION

ELECTROMAGNETIC field models that do not account for radiation effects are dubbed quasistatic field models. For static fields, the Maxwell equations decouple and enable the consideration of resistive, and capacitive or inductive effects, with either electrostatic, or magnetostatic formulations, separately. For capacitive-resistive effects, the electroquasistatic (EQS) field model is applicable, while resistive-inductive effects can be modelled with the magneto-quasistatic (MQS) field approximation [1]. Quasistatic field scenarios where inductive, resistive, and capacitive effects need to be considered simultaneously, appear in high-frequency coils and coils of inductive charging systems, where the capacitive effects between the coil windings need to be taken into account and they are a common problem in electromagnetic compatibility, e.g. in automotive engineering. For such scenarios, it is quite common to use lumped R, L, C parameter circuit-type models such as Kirchhoff's model or circuit models in combination with field models used either for parameter extraction or in strong/weakly coupled models, and circuit-formulation oriented partial-element equivalent circuit (PEEC) methods. Rather recently, also field oriented models based on the Darwin field formulation are considered. These quasistatic electromagnetic field models are represented in terms of combined electric scalar and magnetic vector potentials and feature a modified version of Ampère's law by eliminating the rotational parts of the displacement currents, i.e., by neglecting the radiation effects in the model. Darwin formulations [2] are

not gauge-invariant, and thus, a number of different Darwin model formulations have been considered, [3], [4], [5], [6], [7], [8], [9], [10], and [11]. The paper is organized as follows. After this introduction, Darwin field models with different established gauge conditions are highlighted. In the third section, a Darwin model is presented which allows to use a two-step numerical solution scheme. Section IV is comprised of numerical experiments with the two-step time domain Darwin formulation, and is followed by conclusions.

II. THE DARWIN FIELD MODEL

Darwin or Darwin-type field models for quasistatic electromagnetic field distributions can be obtained by considering a decomposition of the electric field intensity $\boldsymbol{E}$ into an irrotational part $\boldsymbol{E}_{\mathrm{irr}}$ and a remaining part $\boldsymbol{E}_{\mathrm{rem}}$,

$$\boldsymbol{E} = \boldsymbol{E}_{\mathrm{irr}} + \boldsymbol{E}_{\mathrm{rem}}, \tag{1}$$

where the irrotational part is represented as the gradient of an electric scalar potential φ, that is, $\boldsymbol{E}_{\mathrm{irr}} = -\operatorname{grad}\varphi$. The remainder part is represented by the time derivative of a magnetic vector potential $\boldsymbol{A}$, i.e., $\boldsymbol{E}_{\mathrm{rem}} = -\partial\boldsymbol{A}/\partial t$. Hence,

$$\boldsymbol{E} = -\frac{\partial}{\partial t}\boldsymbol{A} - \operatorname{grad}\varphi, \qquad \boldsymbol{B} = \operatorname{curl}\boldsymbol{A} \tag{2}$$

holds for the electric field intensity and for the magnetic flux density, respectively.

The assumption of a quasistatic electromagnetic field model enables the elimination of the rotational parts of the displacement currents, $\varepsilon\partial^2\boldsymbol{A}/\partial t^2 \cong \boldsymbol{0}$, in Ampère's law. The result of this elimination is the so-called Darwin-Ampère equation

$$\operatorname{curl}(\nu\operatorname{curl}\boldsymbol{A}) + \kappa\frac{\partial}{\partial t}\boldsymbol{A} + \kappa\operatorname{grad}\varphi + \varepsilon\operatorname{grad}\frac{\partial}{\partial t}\varphi = \boldsymbol{J}_{\mathrm{S}}, \tag{3}$$

where ν is the reluctivity, κ is the electric conductivity, ε is the permittivity, and $\boldsymbol{J}_{\mathrm{S}}$ is a source current density.

The original formulation of the Darwin model [2] can be obtained by enforcing a Coulomb gauge $\operatorname{div}(\boldsymbol{A}) = 0$ corresponding to a Helmholtz decomposition of the electric field intensity $\boldsymbol{E}$, i.e., assuming $\operatorname{curl}\boldsymbol{E}_{\mathrm{irr}} = 0$ and $\operatorname{div}\boldsymbol{E}_{\mathrm{rem}} = -\operatorname{div}(\partial\boldsymbol{A}/\partial t) = 0$. Intended to model charges in free space without conductive materials, i.e., $\kappa = 0$, $\varepsilon = \varepsilon_0$ and $\nu = \nu_0$, as a consequence to the Helmholtz decomposition, the Gauß law does not consider the rotational parts of the electric field and yields the electrostatic Poisson equation as a gauge

equation. Thus, the original Darwin formulation is given by

$$-\nu_0 \Delta \boldsymbol{A} + \varepsilon \operatorname{grad} \frac{\partial}{\partial t}\varphi = \boldsymbol{J}_{\mathrm{S}}, \quad (4)$$

$$\operatorname{div} \operatorname{grad} \varphi = -\rho_{\mathrm{E}}/\varepsilon_0, \quad (5)$$

which requires to know the electric charge density ρ_{E} and its motion with $\boldsymbol{J}_{\mathrm{S}} = \rho_{\mathrm{E}}\boldsymbol{v}$ along some velocity vector $\boldsymbol{v}$.

To eliminate the free space assumption of the original Darwin model and to include conductors, and permeable and dielectric materials, an application of the divergence operator to the Darwin-Ampère equation (3) results in a modified Darwin field formulation [5], [6], and yields the Darwin continuity equation

$$\operatorname{div}\left(\kappa\frac{\partial}{\partial t}\boldsymbol{A} + \kappa\operatorname{grad}\varphi + \varepsilon\operatorname{grad}\frac{\partial}{\partial t}\varphi\right) = \operatorname{div}\boldsymbol{J}_{\mathrm{S}}. \quad (6)$$

This Darwin continuity equation lacks the radiation term $\operatorname{div}(\varepsilon\partial^2\boldsymbol{A}/\partial t^2)$, which is present in the full Maxwell continuity equation. It was shown [5] that the combined discrete formulation of the Darwin-Ampère equation (3) and the Darwin continuity equation (6) results in non-symmetric systems. In addition, the resulting system is singular and requires an additional gauge for the magnetic vector potential in the non-conductive regions of the problem, such as artificial conductivity [5] or an additional Coulomb-type gauge [8], [11]

$$\operatorname{div}\left(\varepsilon\frac{\partial}{\partial t}\boldsymbol{A}\right) = 0, \quad (7)$$

which can be enforced by adding this term with a scaling factor $1/\Delta t$ to the Darwin continuity equation (6), such that the gauge equation becomes a temporally semi-discrete version of the full Maxwell continuity equation, expressed in terms of the electrodynamic potentials $\boldsymbol{A}$ and φ. The Coulomb-type gauge (7) can be additionally imposed as a third equation via a Lagrange multiplier formulation [8]. Both Darwin model field formulations, [8] and [11], are symmetric and do not require additional regularization.

III. TWO-STEP DARWIN MODEL ALGORITHMS

The Darwin continuity equation (6) is extended with an additional gauge term $\operatorname{div}(\kappa\partial\boldsymbol{A}/\partial t) = 0$ [10] to yield the electro-quasistatic equation

$$\operatorname{div}\left(\kappa\operatorname{grad}\varphi + \varepsilon\operatorname{grad}\frac{\partial}{\partial t}\varphi\right) = \operatorname{div}\boldsymbol{J}_{\mathrm{S}}. \quad (8)$$

The expression $\operatorname{div}(\kappa\partial\boldsymbol{A}/\partial t)$ omitted in (8) from the Darwin continuity equation (6), corresponds to explicitly enforcing divergence-free eddy currents in conductive media, i.e., neglecting eventually arising sources and sinks of current densities due to the irrotational parts of the electric field. The combination of equation (3) rewritten as

$$\operatorname{curl}(\nu\operatorname{curl}\boldsymbol{A}) + \kappa\frac{\partial}{\partial t}\boldsymbol{A} = -\kappa\operatorname{grad}\varphi - \varepsilon\operatorname{grad}\frac{\partial}{\partial t}\varphi + \boldsymbol{J}_{\mathrm{S}}, \quad (9)$$

with equation (8) results in a two-step formulation, where first the electro-quasistatic total current density $\boldsymbol{J}_{\mathrm{total}} = -\kappa\operatorname{grad}\varphi - \varepsilon\operatorname{grad}(\partial\varphi/\partial t) + \boldsymbol{J}_{\mathrm{S}}$ is used as a solenoidal source term with $\operatorname{div}\boldsymbol{J}_{\mathrm{Total}} = 0$ to a magneto-quasistatic formulation for the magnetic vector potential $\boldsymbol{A}$ represented by the lefthand

side of (9). This modified magneto-quasistatic formulation, however, initially does not not address irrotational parts of $\boldsymbol{A}$ in the non-conductive regions. While this does not affect the evaluation of $\boldsymbol{B}$ in (2), the evaluation of the electric field according to (2) involves the expression $\partial\boldsymbol{A}/\partial t$ also in the non-conductive regions, which is commonly not covered in magneto-quasistatic field formulations.

To control the irrotational parts of $\boldsymbol{A}$, the magneto-quasistatic formulation needs to be regularized. For this, the introduction of a small artificial electrical conductivity $\hat{\kappa}$ in the non-conducting regions has been suggested [5]. In case that $\kappa \gg 1/(\Delta t)\varepsilon$ holds for a given time-step length Δt, a modified electrical conductivity as e.g. $\hat{\kappa} = \kappa + 1/(\Delta t)\varepsilon$ will regularize the formulation, where the resulting time-discrete formulations will feature expressions of the type $1/(\Delta t)\kappa + 1/(\Delta t)^2\varepsilon$ as they occur in second-order time discretization schemes, as e.g. Newmark-beta schemes used for full wave Maxwell-Ampère equations [12]. Alternatively, a grad-div term augmentation for spatially discretized magneto-quasistatic formulations is applicable [13], [14].

The introduction of a small artificial electrical conductivity $\hat{\kappa}$ in the non-conducting regions is also an established technique to mitigate the static limit instability of the electro-quasistatic formulation (8) that is known to occur for $\frac{\partial}{\partial t}\varphi \to 0$.

By assuming that $\operatorname{div}(\kappa\partial\boldsymbol{A}/\partial t) = 0$ holds in equation (6), the calculation of the electric scalar potential φ, using (8), is decoupled from that of the magnetic vector potential $\boldsymbol{A}$. Thus, it is possible to independently first solve an electro-quasistatic initial-boundary value problem that corresponds to (8), and in a second step solve the modified magneto-quasistatic problem (9) with the then available total current densities $\boldsymbol{J}_{\mathrm{Total}}$, as depicted in Algorithm 1.

Algorithm 1 Two-Step Darwin Time Domain

1: Initialize $\varphi(t^0)$ and $\boldsymbol{A}(t^0)$;
2: **for** $n \leftarrow 0 : n_{\mathrm{End}} - 1$ **do**
3:      Solve problem (8) for $\varphi(t^{n+1})$;
4: **end for**
5: **for** $n \leftarrow 0 : n_{\mathrm{End}} - 1$ **do**
6:      Solve problem (9) for $\boldsymbol{A}(t^{n+1})$;
7:      Evaluate $\boldsymbol{E}(t^{n+1})$ and $\boldsymbol{B}(t^{n+1})$ with (2);
8: **end for**

Alternatively, it is possible to consecutively execute a solution step for an electro-quasistatic and a magneto-quasistatic field formulation for each discrete timestep, using suitable time stepping schemes [15].

A. Discrete Two-Step Darwin Time Domain Schemes

Reformulating (6) and (9) with a spatial volume discretization scheme, such as the finite integration technique [16] or the finite element method with Nédélec elements [17], results in a coupled system of time continuous matrix equations

$$\mathbf{G}^\top\mathbf{M}_\kappa\mathbf{G}\boldsymbol{\phi} + \mathbf{G}^\top\mathbf{M}_\varepsilon\mathbf{G}\frac{\mathrm{d}}{\mathrm{d}t}\boldsymbol{\phi} = \mathbf{G}^\top\mathbf{j}_{\mathrm{s}} - \mathbf{G}^\top\mathbf{M}_\kappa\frac{\mathrm{d}}{\mathrm{d}t}\mathbf{a}, \quad (10)$$

$$\mathbf{C}^\top\mathbf{M}_\nu\mathbf{C}\mathbf{a} + \mathbf{M}_\kappa\frac{\mathrm{d}}{\mathrm{d}t}\mathbf{a} = \mathbf{j}_{\mathrm{s}} - \mathbf{M}_\kappa\mathbf{G}\boldsymbol{\phi} - \mathbf{M}_\varepsilon\mathbf{G}\frac{\mathrm{d}}{\mathrm{d}t}\boldsymbol{\phi}, \quad (11)$$

where $\mathbf{a}$ is the degrees of freedom (dof) vector related to the magnetic vector potential, $\boldsymbol{\phi}$ is the dof vector of electric nodal scalar potentials, $\mathbf{j}_s$ is a vector of transient source currents, $\mathbf{C}$ is the discrete curl operator matrix, $\mathbf{G}$ and $\mathbf{G}^\top$ are discrete gradient and (negative) divergence operator matrices. The matrices $\mathbf{M}_\nu$, $\mathbf{M}_\kappa$, $\mathbf{M}_\varepsilon$ are discrete material matrices of possibly nonlinear reluctivities, conductivities and permittivities, respectively, corresponding to the specific discretization scheme in use. Employing e.g. an implicit Euler backward differentiation time stepping scheme with time step Δt to (10) and (11) and $\mathbf{M}_\sigma = \mathbf{M}_\kappa + (1/\Delta t)\mathbf{M}_\varepsilon$ yields a coupled system

$$\left[\mathbf{G}^\top \mathbf{M}_\sigma \mathbf{G}\right] \boldsymbol{\phi}^{n+1} = \mathbf{f}_1(\mathbf{a}^{n+1}), \tag{12}$$

$$\left[\mathbf{C}^\top \mathbf{M}_\nu \mathbf{C} + \frac{1}{\Delta t}\mathbf{M}_\kappa\right]\mathbf{a}^{n+1} = \mathbf{f}_2(\boldsymbol{\phi}^{n+1}), \tag{13}$$

where, using the notation $\Delta\mathbf{a}^{n+1} = \mathbf{a}^{n+1} - \mathbf{a}^n$, the right-hand side vectors are

$$\mathbf{f}_1 = \mathbf{G}^\top \mathbf{j}_s^{n+1} + \frac{1}{\Delta t}\mathbf{G}^\top \mathbf{M}_\varepsilon \mathbf{G}\boldsymbol{\phi}^n - \frac{1}{\Delta t}\mathbf{G}^\top \mathbf{M}_\kappa \Delta\mathbf{a}^{n+1}, \tag{14}$$

$$\mathbf{f}_2 = \mathbf{j}_s^{n+1} + \frac{1}{\Delta t}\mathbf{M}_\kappa \mathbf{a}^n - \mathbf{M}_\sigma \mathbf{G}\boldsymbol{\phi}^{n+1} + \frac{1}{\Delta t}\mathbf{M}_\varepsilon \mathbf{G}\boldsymbol{\phi}^n. \tag{15}$$

System (12), (13) are solved for each time step, starting from initial values $\mathbf{a}^0 = \mathbf{a}(t^0)$ and $\boldsymbol{\phi}^0 = \boldsymbol{\phi}(t^0)$. Adopting an iterative solution approach with iteration index $i = 0, 1, 2, \ldots$ for each time step t^{n+1} requires to provide an initial guess vector $\mathbf{a}_{i=0}^{n+1}$ with $\mathbf{f}_{1,i=0} = \mathbf{f}_1(\mathbf{a}_{i=0}^{n+1})$. Inserting the solution vector of (12) rewritten as $\boldsymbol{\phi}^{n+1} = \left[\mathbf{G}^\top \mathbf{M}_\sigma \mathbf{G}\right]^{-1} \mathbf{f}_{1,i=0}$ into the right-hand side vector equation $\mathbf{f}_{2,i=0} = \mathbf{f}_2(\boldsymbol{\phi}_{i=0}^{n+1})$ of (13) yields an expression for the next iterative solution vector $\mathbf{a}_{i=1}^{n+1}$. Left application of the discrete divergence operator $\mathbf{G}^\top$ to this equation using the relation $\mathbf{G}^\top \mathbf{C}^\top = \mathbf{0}$ yields the identity $\mathbf{G}^\top \mathbf{M}_\kappa \mathbf{a}_{i=1}^{n+1} = \mathbf{G}^\top \mathbf{M}_\kappa \mathbf{a}_{i=0}^{n+1}$ and by induction

$$\mathbf{G}^\top \mathbf{M}_\kappa \mathbf{a}_i^{n+1} = \mathbf{G}^\top \mathbf{M}_\kappa \mathbf{a}_0^{n+1} \quad \forall i \in \{0, 1, \ldots\}, \tag{16}$$

i.e., in exact arithmetics the converged solution $\mathbf{a}^{n+1}$ of the iterative process will maintain the discrete divergence of its initial guess solution $\mathbf{a}_{i=0}^{n+1}$ in the right-hand side (14) of (12). An initial guess $\mathbf{a}_{i=0}^{n+1} = \mathbf{a}^n$ yields the result

$$\mathbf{G}^\top \mathbf{M}_\kappa \mathbf{a}^n = \mathbf{G}^\top \mathbf{M}_\kappa \mathbf{a}^0 \quad \forall n \in \{0, 1, \ldots\}. \tag{17}$$

Thus, with the choice of the initialization vector $\mathbf{a}^0$ of the time integration process at t^0 acting as an initial gauge, the difference expression $\mathbf{G}^\top \mathbf{M}_\kappa \left[\mathbf{a}^{n+1} - \mathbf{a}^n\right] = \mathbf{0}$ in (14) vanishes for all time steps, and thus, system (12), (13) gets decoupled.

IV. NUMERICAL EXPERIMENTS

To verify the performance of the proposed two-step Darwin time domain algorithm, two three-dimensional copper coil problems are considered (electrical conductivity $\kappa_{\text{copper}}, = 5.96 \cdot 10^7$ S/m. Both problems are illustrated in Fig. 1. For each case-study, the computational domain is $\Omega = (\Omega_0 \cup \overline{\Omega}_\kappa) \backslash (\Gamma_E \cup \Gamma_G) \subset \mathbb{R}^3$ and is free from charge and current sources. The bounding surfaces are perfectly conducting, with Γ_G being grounded and Γ_E supplying the transient excitation

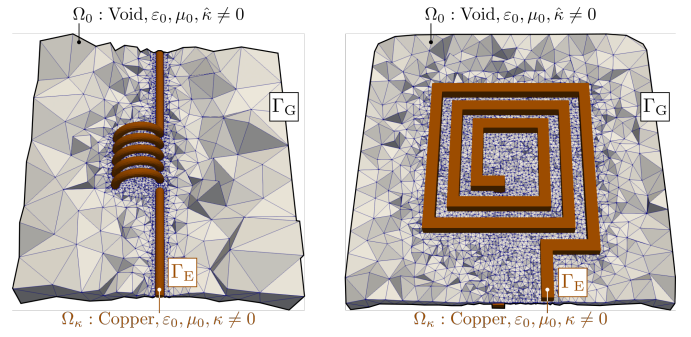$$\varphi(t) = \varphi_{\max} \cdot f \cdot \min(t, 1/f) \cdot \sin(2\pi f t), \tag{18}$$

Fig. 1. In both coil case-studies, Ω_0 is void, with $\hat{\kappa}$ being a small artificial electrical conductivity ($\hat{\kappa} = 10^{-2}$ S/m), while Ω_κ is occupied by copper.

TABLE I
NUMBER OF DEGREES OF FREEDOM (DOF)

	Lagrange Elements	Nédélec Elements
Helical Coil	16 882	118 609
Planar Coil	41 357	292 905

where $\varphi_{\max} = 12$ V is the maximum voltage and $f = 10$ MHz is the excitation frequency with a wavelength $\lambda = 30$ m in void. The longest side of the domain Ω associated with the helical coil is $l = 6.3$ cm, the one associated with the planar coil is $l = 1.35$ cm. Since $\ell \ll \lambda$ in both cases, the radiation-free assumption of the Darwin field model is justified.

The problems that constitute the two-step algorithm are discretized in space with the FEM, using first-order Lagrange elements for the scalar electric problem and zeroth-order Nédélec elements for the vectorial magnetic problem; see Table I for the number of degrees of freedom in each finite element space. Regarding time-discretization, both problems have been integrated with the trapezoidal method, which is implicit, second-order accurate, and A-stable, with different time steps $\Delta t \in \{2.5, 1.25, 0.625\}$ ns for a total of $t_{\text{End}} = (n_{\text{End}} - 1)\Delta t = 1200$ ns. With the excitation functions in (18), the two-step algorithm is expected to yield an approximation of a frequency-domain full Maxwell solution, and hence, the latter is used for obtaining reference solutions on the same meshes. For all linear systems a direct solver is used.

In Fig. 2, the magnetic flux density and the electric field intensity are depicted for each coil. There, the two-step algorithm for the Darwin field model, successfully captures, not only the induction, but also the capacitance between the coil windings. Table II depicts the relative differences of the electric field approximations provided by the Darwin field model for the planar coil model at frequencies ranging from 10 kHz up through 1 GHz. The results show that the remainder part $-\partial \boldsymbol{A}/\partial t$ of the electric field needs to be evaluated in (2) which necessitates the regularization of (9).

In Fig. 3, the difference between the Maxwell and Darwin field models is quantified with the norm

$$\|\operatorname{Re}(\boldsymbol{F}_{\text{M}}) - \boldsymbol{F}_{\text{D}}\|_{L^2(\Omega)} / \|\boldsymbol{F}_{\text{M}}\|_{L^2(\Omega)}, \tag{19}$$

where $\boldsymbol{F} \in \{\boldsymbol{B}, \boldsymbol{E}\}$ is a physical field quantity, computed as in (2), and the subscripts M and D stand for the Maxwell and
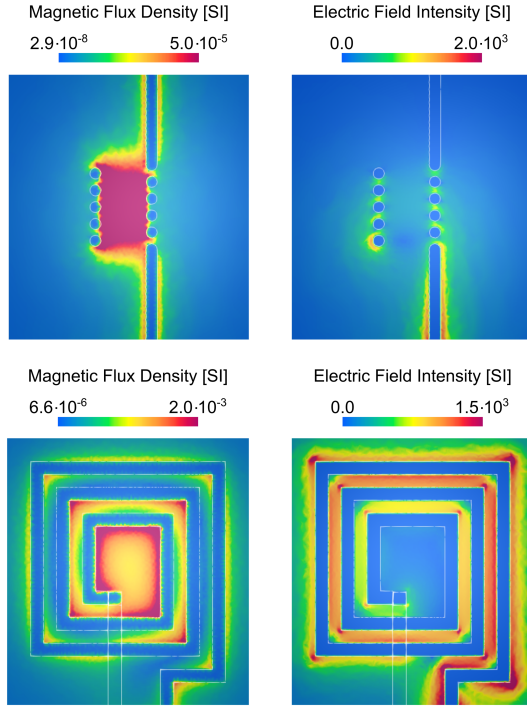
Fig. 2. The magnitude of the magnetic flux density and the electric field intensity for the two coil problems at $t = 825$ ns.
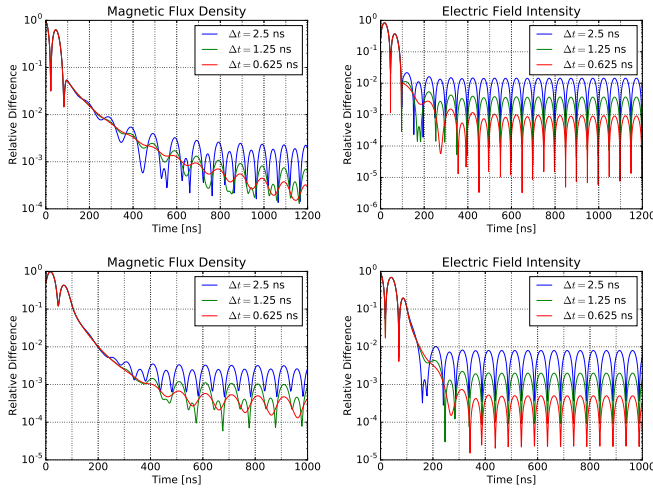

Fig. 3. The relative difference between the field quantities $\boldsymbol{B}$ and $\boldsymbol{E}$ for the helical coil (first row) and for the planar coil (second row), computed using a full Maxwell frequency-domain solver and the two-step Darwin algorithm.

Darwin field models, respectively. In Fig. 3, the first row of results is associated with the helical coil, while the second row with the planar coil. In the same figure, the effect of the time discretization scheme is also apparent, with a tendency towards improved accuracy for smaller time steps, since convergence to the time-harmonic solution is expected.

V. CONCLUSIONS

A two-step algorithm for the transient $(\boldsymbol{A}, \varphi)$ formulation of the quasistatic Darwin field model is introduced and, for the first time, numerically validated against the full system

of Maxwell's equations. The presented two-step Darwin time domain quasistatic field formulation accounts for capacitive, inductive, and resistive effects. The advantages of this scheme result from consecutively combining an electro-quasistatic and a modified magneto-quasistatic field model, and thus, it benefits from existing efficient time domain solution techniques that provide flexibility in terms of material non-linearities and excitation profiles.

TABLE II
RELATIVE $\boldsymbol{E}$-FIELD DIFFERENCES AT $t = 3.125/f$ FOR THE PLANAR
COIL AS FUNCTIONS OF THE FREQUENCY f.

f [Hz]	$\| \mathrm{Re}(\boldsymbol{E}_{\mathrm{M}}) - \boldsymbol{E}_{\mathrm{D}}\|/\|\boldsymbol{E}_{\mathrm{M}}\|$	$\| \mathrm{Re}(\boldsymbol{E}_{\mathrm{M}}) - \boldsymbol{E}_{\mathrm{D,irr}}\|/\|\boldsymbol{E}_{\mathrm{M}}\|$
10^4	$8.22 \cdot 10^{-6}$	$2.74 \cdot 10^{-3}$
10^5	$9.31 \cdot 10^{-6}$	$2.92 \cdot 10^{-2}$
10^6	$4.60 \cdot 10^{-5}$	$1.59 \cdot 10^{-1}$
10^7	$7.33 \cdot 10^{-4}$	1.47
10^8	$2.00 \cdot 10^{-3}$	2.28
10^9	$1.41 \cdot 10^{-2}$	2.22

REFERENCES

[1] H. A. Haus and J. R. Melcher, *Electromagnetic Fields and Energy*. Englewood Cliffs, New Jersey: Prentice Hall, 1989.

[2] C. G. Darwin, "The dynamical motion of particles," *Phil. Mag.*, vol. 93, pp. 537 – 551, 1920.

[3] P. A. Raviart and E. Sonnendrücker, "Approximate models for the Maxwell equations," *J. Comp. Appl. Math.*, vol. 63, pp. 69 – 81, 1995.

[4] J. Larsson, "Electromagnetics from a quasistatic perspective," *Am. J. Phys.*, vol. 75, no. 3, pp. 230–239, 1995.

[5] S. Koch and T. Weiland, "Different types of quasistationary formulations for time domain simulations," *Radio Science*, vol. 46, 2011.

[6] S. Koch, H. Schneider, and T. Weiland, "A low-frequency approximation to the Maxwell equations simultaneously considering inductive and capacitive phenomena," *IEEE Trans. Magn.*, vol. 48, no. 2, pp. 511–514, 2012.

[7] I. C. Garcia, S. Schöps, H. D. Gersem, and S. Baumanns, "Chapter 1 systems of differential algebraic equations in computational electromagnetics," in *Applications of Differential-Algebraic Equations: Examples and Benchmarks* (S. Campell, A. Ilchmann, V. Mehrmann, and T. Reis, eds.), pp. 123–169, Springer Verlag, 2018.

[8] Y. Zhao and Z. Tang, "A novel gauged potential formulation for 3d electromagnetic field analysis including both inductive and capacitive effects," *IEEE Trans Magn.*, vol. 55, pp. 1–5, June 2019.

[9] Z. Badics, S. Bilicz, J. Pávo, and S. Gyimóthy, "Finite element a − v formulations for quasistatic Darwin models," in *Proc. IEEE CEFC 2018 Conference, Hangzhou, China*, 2018.

[10] M. Clemens, B. Kähne, and S. Schöps, "A Darwin time domain scheme for the simulation of transient quasistatic electromagnetic fields including resistive, capacitive and inductive effects," in *2019 Kleinheubach Conference, Miltenberg, Germany*, pp. 1–4, 2019.

[11] H. Kaimori, T. Mufune, and A. Kameari, "Novel application of Coulomb gauge condition in electromagnetic fem computations for Darwin approximation," in *IEEE CEFC 2020 Conference, Pisa, Italy*, p. 497, 2020.

[12] D. C. Dibben and R. Metaxas, "Frequency domain vs. time-domain finite element methods for calculation of fields in multimode cavities," *IEEE Trans. Magn.*, vol. 33, no. 2, pp. 1468–1471, 1997.

[13] A. Bossavit, "'Stiff' problems in eddy-current theory and the regularization of Maxwell's equations," *IEEE Trans. Magn.*, vol. 37, pp. 3542–3545, Sept. 2001.

[14] M. Clemens, S. Schöps, H. De Gersem, and A. Bartel, "Decomposition and regularization of nonlinear anisotropic curl-curl daes," *COMPEL*, vol. Vol. 30, no. No. 6, pp. 1701–1714, 2011.

[15] M. Clemens, "Large systems of equations in a discrete electromagnetism: Formulations and numerical algorithms," *IEE Proc. - Scie. Meas. Technol.*, vol. 152, no. 2, pp. 50–72, 2005.

[16] T. Weiland, "Time domain electromagnetic field computation with finite difference methods," *Int. J. Num. Mod.: ENDF*, vol. 9, pp. 259–319, 1996.

[17] J. C. Nédélec, "Mixed finite elements in R^3," *Numer. Math.*, vol. 35, pp. 315–341, 1980.